Materials Research Proceedings 41 (2024) 1867-1876 https://doi.org/10.21741/9781644903131-207

An innovative method to model run-out phenomena in micro-milling by using cutting force signal

SENECI Greta[1,a], PANCERA Pierpaolo Vincenzo[1,b], CAPPELLINI Cristian[2,c], ABENI Andrea[1,d*] and ATTANASIO Aldo[1,e]

[1]Department of Mechanical and Industrial Engineering, University of Brescia, Via Branze 38, 25123 Brescia, Italy

[2]Department of Management, Information and Production Engineering, University of Bergamo, Via Pasubio 7/b, 24044 Dalmine, Italy

[a]greta.seneci@unibs.it, [b]p.pancera001@studenti.unibs.it, [c]cristian.cappellini@unibg.it, [d]andrea.abeni@unibs.it, [e]aldo.attanasio@unibs.it

Keywords: Tool Run-Out, Micro-Milling, Al-Si-10mg, Analytical Modeling, Additive Manufacturing

Abstract. This work deals with the modeling of micro-milling processes by considering the phenomena generated by the transition from conventional size to the micro-scale machining. The concomitant effects of different cutting regimes, and the deviation of the cutting edges from their theoretical trajectories due to tool run-out, are important aspects to be considered during the process modeling. Several models are available in literature to describe how ploughing and shearing regimes influence cutting forces and how the tool run-out impacts on the actual chip thickness. In a previous authors research, a comprehensive model was published achieving a good agreement with the experimental data, but its calibration requires the measurement of the width of the micro-milled slots. This practice is time consuming and subjected to experimental errors, while a calibration of the model based only on the elaboration of the cutting force signal appears a promising strategy. Starting from the mathematical description of the geometrical model, a new equation to compute the tool run-out parameters was found. The parameters depend on eight variables that must be calculated from tool geometry, material composition, cutting parameters and the cutting force signal. An experimental procedure was developed to compare the prediction achieved by the new method and the conventional technique.

Introduction

Micro-milling is a machining operation concerning the employment of cutting tools with a diameter lower than 1 mm. At this scale level, critical issues, usually neglectable when dealing with the same process on conventional scale, rise up. These issues are size effect, burr formation, high cutting forces, rapid tool wear, different cutting regimes (*ploughing* and *shearing*) and tool run-out [1, 2]. Ploughing regime is an undesired cutting condition in which uncut chip thickness is not sufficient to completely remove the chip and a not-neglectable elastic deformation is induced in the workpiece. This phenomenon implicates the increase of cutting forces as well as a poor surface quality on the machined features [3]. On the contrary, when chip thickness is higher than a threshold value, i.e. Minimum Uncut Chip Thickness (MUCT), shearing regime occurs. The uncut chip thickness depends on the instantaneous trajectories of the tool cutting edges, which are strongly influenced by tool run-out. This latter is defined as the deviation of the effective tool's rotational axis from the theoretical one. The phenomenon implicates different uncut chip thickness in relation of each cutting edge. Therefore, different cutting forces are applied on each tool flute, with a resulting non-homogeneous tool wear. So that, many researchers focused on considering tool run-out and cutting regimes when modelling micro-milling [4, 5].

Bissacco et al. [6] proposed an analytical model to estimate the unbalancing of cutting forces due to tool run-out. In this model, different force profiles for each cutting edge are considered as a function of tool run-out. Rodriguez & Labarga [7] elaborated an analytical force model through a set of linear equations considering the run-out deviation, the tool deflection and the size effect. Chen et al. [8] proposed an analytical model that considers both ploughing and shearing conditions depending on the value of uncut chip thickness. The instantaneous uncut chip thickness was calculated by considering tool run-out and the machine tool systems vibrations. Many experimental tests confirmed the capability of the model to provide an accurate force prediction. A similar model was elaborated by Zhang et al. [9]. This model was validated by performing a series of micro end milling experiments on Al6061 workpieces under different conditions.

The purpose of this paper is to verify a novel procedure to quantify tool run-out through the model described in [5], by only exploiting the cutting force signal as model input. An experimental method was defined to compute the unknown parameters of the geometrical model of run-out. Firstly, micro-channels were realized on AlSi10Mg samples fabricated with different production technologies (i.e., additive manufacturing and casting). The tests were performed by varying the feed rates in order to change the chip cross section to investigate the cutting regime transition. During the process, the cutting force was acquired using a load cell. After the process, channel's width was measured with a profilometer laser probe and data were used to calibrate the model described in [5]. Finally, the experimental outputs were compared with the results of the innovative calibration procedure to assess its reliability.

Tool run-out model

Fig. 1a represents the run-out effect on the tool flutes trajectories and the related geometric parameters. The analysis considers for simplicity a two cutting edges tool, which is sectioned in a plane normal to the theoretical tool rotation axis. Tool run-out has three main effects on the cutting process:

1. The effective radius of one of the cutting edges, in this investigation the first one (r_{CE1}), increases.
2. The radius of the other cutting edge, in this study the second one (r_{CE2}), decreases.
3. The phase angle α [rad] between the two cutting edges is not constantly equal to π [rad].

The run-out can be evaluated using two geometric parameters: the run-out length r_0, defined as the distance between the theoretical spindle rotational centre O and the effective one O'; and the run-out angle γ as represented in Fig. 1. Even though these parameters cannot be directly measured, it is demonstrated [10] that they can be estimated assessing the tool diameter d [mm], the cutting-edge phase angle α [rad] and the rotational radius of the main cutting edge r_{CE1} [mm], by applying Eq. 1 and Eq. 2:

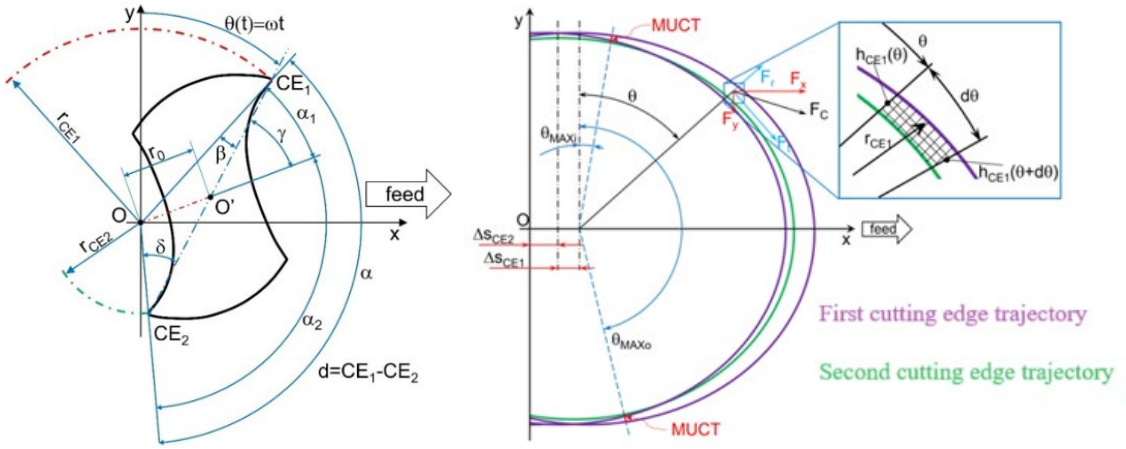

*Figure 1 – (**a**) Geometrical representation of tool run-out (**b**) and representation of tool edge trajectories and force components.*

$$r_0 = \sqrt{{r_{CE2}}^2 + \left(\frac{d}{2}\right)^2 - 2 \cdot r_{CE2} \cdot \frac{d}{2} \cdot \cos\delta} \tag{1}$$

$$\gamma = \arcsin\left(\frac{r_{CE2}}{r_0} \cdot \sin\delta\right) \tag{2}$$

where angle δ and r_{CE2} are again expressed as a function of the previously reported measurable parameters (Eq. 3 and Eq. 4) [10]:

$$\delta = \arcsin\left(\frac{r_{CE1}}{d} \cdot \sin\alpha\right) \tag{3}$$

$$r_{CE1} = \sqrt{r_{CE1}^2 + d^2 - 2 r_{CE1} d\, cos(\pi - \alpha - \delta)} \tag{4}$$

In [10] the whole procedure for determining the phase angle α, using the cutting period derived from the force signal, and for measuring d and r_{CE1} is clearly explained.

In Fig. 1b it is possible to see how the run-out influence the trajectories of the tool flutes and its effect on the instantaneous uncut chip thickness h.

The total cutting force F_C is the combination of its spatial components F_x, F_y, and F_z. In turn, the F_C component in the section plane can be subdivided in its tangential F_t and radial F_r components as demonstrated in [5]. They depend on tool rotational angle θ and they can be decomposed along x-axis and y-axis by using the set of Eqs. 5, where the subscripted number is related to the considered cutting edge.

$$\begin{cases} F_{x1} = F_{t1} \cdot cos\,\theta + F_{r1} \cdot sin\,\theta \\ F_{y1} = -F_{t1} \cdot sin\,\theta + F_{r1} \cdot cos\,\theta \\ F_{x2} = F_{t2} \cdot cos\,\theta + F_{r2} \cdot sin\,\theta \\ F_{y2} = -F_{t2} \cdot sin\,\theta + F_{r2} \cdot cos\,\theta \end{cases} \tag{5}$$

As developed in [5], for each cutting edge, tangential and radial force components can be estimated by the set of Eqs. 6 as follows:

$$\begin{cases} F_{t1}(\theta) = \left(K_{ts} \cdot h_{CE1}(\theta) + K_{tp} \cdot A_{p1}(\theta)\right) \cdot a_p \\ F_{r1}(\theta) = \left(K_{rs} \cdot h_{CE1}(\theta) + K_{rp} \cdot A_{p1}(\theta)\right) \cdot a_p \\ F_{t2}(\theta) = \left(K_{ts} \cdot h_{CE2}(\theta) + K_{tp} \cdot A_{p2}(\theta)\right) \cdot a_p \\ F_{r2}(\theta) = \left(K_{rs} \cdot h_{CE2}(\theta) + K_{rp} \cdot A_{p2}(\theta)\right) \cdot a_p \end{cases} \quad (6)$$

where K_{ts} [N/mm^2], K_{tp} [N/mm^3], K_{rs} [N/mm^2], and K_{rp} [N/mm^3] are tangential and radial specific cutting force coefficients for shearing and ploughing regime respectively, and they depend on workpiece material; $h_{CE1}(\theta)$ [mm] and $h_{CE2}(\theta)$ [mm] are the chip thicknesses, as a function of the tool rotational angle, for the first and the second cutting edge respectively; a_p [mm] is the axial depth of cut; and A_p [mm^2] is the ploughed area, computed as the portion of the cut material which remain in ploughing regime due to the low value of chip thickness.

Considering that the peaks force of each cutting edge will be in correspondence of maximum chip cross-sectional area, for the first Cutting Edge (*CE1*) the peak occurs when $\theta \approx 90°$, while for the second Cutting Edge (*CE2*) the peak will appear at $\theta \approx 270°$. Fig. 2a shows an example of the force trend in the direction orthogonal to the feed direction (F_y) during angle θ variation. The difference between the peaks of the force amongst the two cutting edges (ΔFy) is visible. Substituting Eqs. 6 in Eqs. 5, and introducing the values of θ in the correspondence of the peaks of the forces, it is possible to define a new equation (Eq. 7) to calculate the force difference in the y-axis between the two cutting edges ΔFy.

$$\frac{\Delta Fy(\theta)}{a_p} = K_{ts}\left(h_{CE1}(\theta) - h_{CE2}(\theta)\right) + K_{tp}\left(A_{pCE1}(\theta) - A_{pCE2}(\theta)\right) \quad (7)$$

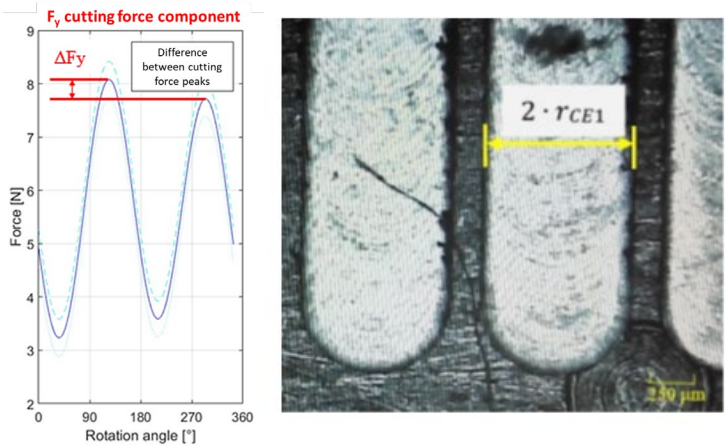

(a) **(b)**

*Figure 2 – (**a**) Trend of cutting force (Fy) vs tool rotational angle (θ) and (**b**) Measure of r_{CE1}.*

If the maximum values of h_{CE1} and h_{CE2} are higher than Minimum Uncut Chip Thickness (*MUCT*), the transition between ploughing and shearing is completely occurred and the ploughing area A_p of the two cutting edges are approximately the same ($A_{pCE1} = A_{pCE2}$). For this reason, Eq. 7 can be simplified in Eq. 8:

$$\frac{\Delta Fy}{a_p} = K_{ts}(h_{CE1}(\theta) - h_{CE2}(\theta)) \quad (8)$$

Referring to Fig. 1b, as reported in [5], h_{CE1} and h_{CE2} are calculated by the set of Eqs. 9:

$$\begin{cases} h_{CE1}(\theta) = \sqrt{(r_{CE1}\sin\theta + \Delta s_{CE1})^2 + (r_{CE1}\cos\theta)^2} - r_{CE2} \\ h_{CE2}(\theta) = \sqrt{(r_{CE2}\sin\theta + \Delta s_{CE2})^2 + (r_{CE2}\cos\theta)^2} - r_{CE1} \end{cases} \quad (9)$$

where Δs_{CE1} is defined as the distance crossed by the rotational axis between the passage of the second cutting edge *CE2* and the consecutive passage of the first one *CE1* in the instantaneous angular position θ, while Δs_{CE2} is the distance crossed between the passage of *CE1* and the consecutive passage of *CE2* (expressed by the set of Eqs. 10).

$$\begin{cases} \Delta s_{CE1} = \frac{f}{60} \cdot \frac{\alpha}{\omega} \\ \Delta s_{CE2} = \frac{f}{60} \cdot \frac{2\pi - \alpha}{\omega} \end{cases} \quad (10)$$

When $\theta \approx 90°$ and $\theta \approx 270°$, substituting the set of Eqs. 9 in Eq. 8, this latter can be rewritten as Eq. 11:

$$\frac{\Delta Fy}{K_{ts} \cdot a_p} = 2 \cdot (r_{CE1} - r_{CE2}) + \Delta s_{CE1} - \Delta s_{CE2} \quad (11)$$

Considering then the set of Eqs. 10, Eq. 11 can be simplified in Eq. 12:

$$r_{CE1} - r_{CE2} = \frac{\Delta Fy}{2 \cdot K_{ts} \cdot a_p} - \frac{f}{60 \cdot \omega}(\alpha - \pi) = I \quad (12)$$

The difference between the two cutting radii is named as *I*. Substituting in Eq. 12 the values of r_{CE2} and β (i.e. π-α-δ), a 4th grade equation to estimate r_{CE1} is found (Eq. 13):

$$a \cdot {r_{CE1}}^4 + b \cdot {r_{CE1}}^3 + c \cdot {r_{CE1}}^2 + e \cdot r_{CE1} + g = 0 \quad (13)$$

Where the parameters *a*, *b*, *c*, *e*, and *g* are computed with Eqs. 14-18:

$$a = sin^4(\alpha) + cos^2(\alpha) \cdot sin^2(\alpha) \quad (14)$$

$$b = -2 \cdot I \cdot sin^2(\alpha) \quad (15)$$

$$c = I^2 + I^2 \cdot sin^2(\alpha) - d^2 \cdot sin^2(\alpha) - d^2 \cdot cos^2(\alpha) \quad (16)$$

$$e = I \cdot d^2 - I^3 \quad (17)$$

$$g = \left(\frac{I^2}{2} - \frac{d^2}{2}\right)^2 \quad (18)$$

All the variables of Eq. 13 can be experimentally determined. The conventional calibration method of the model, described in [5], requires the direct measurement of the micro-slots widths to establish the experimental value of r_{CE1}, assuming that their widths are equal to the double of r_{CE1} (see Fig. 1 and Fig. 2b). The resolution of the Eq. 13 would allow to estimate the value of r_{CE1} only by measuring the difference between the force peaks with the undirect method. Once r_{CE1} is known, all the other geometrical parameters, including r_0 and γ, can be calculated without any dimensional measurement of the micro-slots. If the value of r_{CE1} obtained by solving the equation would be coherent with the experimental one, the model could be employed to estimate tool run-out. This would consent to avoid channels measurements in the experimental procedure and

conclude that the determination of tool run-out would be possible only basing on cutting forces analysis.

Material and methods

The experimental validation of the new method was performed by micro-milling of AlSi10Mg prismatic specimens in two different furnishing conditions. The first one was fabricated by Laser Based Powder Bed Fusion (LB-PBF) and treated with HIP and T6. The LB-PBF samples were produced using the laser-based powder bed fusion machine EOSM290 machine. The process parameters were: a laser power of 370 W, a scanning speed of 1300 mm/s, a hatching distance of 190 µm, a layer thickness of 30 µm, a temperature of the building platform equal to 80 °C. The second one was obtained by Gravity Casting (GC) and treated with T6. Table 1 summarizes the chemical composition of the alloys.

Table 1– Chemical composition (wt.%) of AlSi10Mg aluminium produced via GC and LB-PBF.

AlSi10Mg	Si	Fe	Mn	Mg	Cu	Al
GC	9.89	0.51	0.40	0.38	0.21	balance
LB-PBF	10.2	0.21	< 0.02	0.40	< 0.002	balance

The T6 heat-treatment consists of a solution treatment at 540 °C for 7 h, followed by quench in water and artificial aging at 160 °C for 4 h, while HIP mechano-thermal treatment consists of a Hot Isostatic Pressing (HIP) treatment at 520 °C for 2 h. These samples were machined by using a Ø 0.8 mm flat-bottom two-flutes micro-mill to realize micro-slots. The actual diameter of the micro-mill was measured with three repetitions with a multifocal microscope Hirox RH-2000 and its value is d = 789±2 µm. Fourteen micro-slots were realized on each sample changing the feed per tooth f_z between two consecutive slots, from a minimum value of 0.5 µm/tooth to a maximum value 7 µm/tooth, while cutting speed v_c = 80 m/min and axial depth a_p = 0.25 mm were kept constant. Moreover, the specimens were bounded to a load cell Kistler 9317C to measure cutting forces. A laser profilometer probe Mitaka PF60 was employed to measure the widths of micro-slots; in Table 2 its main properties are listed.

Table 2 – Laser profilometer properties.

Property	Value
Range measurement [mm]	60x60x10
x, y resolution [µm]	0.1
z resolution [µm]	0.01
Laser spot diameter [µm]	1
Laser wavelength [nm]	635

The laser scanning speed was 20 µm/s and the measuring software was MitakaMap. As the mean micro-slot length is about 4500 µm, a measure has been made every 1125 µm to estimate the width. Therefore, the laser probe was employed to execute five profile scans for each micro-slot. In some cases, the excessive burr does not allow to measure the width properly. For this reason, the novel procedure to estimate run-out was tested only on the micro-slots with an average width W_{av} higher than d = 789 µm. The values of r_{CE1} are calculated as half of the W_{av}. A Matlab script was defined to estimate the difference between the two cutting force peaks detected during

the process in the y-direction. The cutting-edge phase angle α can be calculated from cutting force signal as reported in [10].

Results and discussion

In the first part of this section the experimental results are presented together with the calculation of the run-out parameters. In the second part, a simplification of Eq. 13 from a 4th grade equation to a 2nd grade equation is carried out. In the last part of the chapter, the simplified analytical model proposed in this work is applied to the case study and a comparison between the values of r_{CE1} experimentally determinate and computed through analytical model is proposed.

This section collects the experimental values of r_{CE1}, the computed values of ΔF_y and α, and the run-out parameters r_0 and γ computed by using equations Eq. 1 and Eq. 2. Table 3 lists the parameters for GC specimen, while Table 4 refers to LB-PBF specimen.

Table 3 – Measures of r_{CE1}, ΔFy and α on GC specimen.

TEST	f_z [mm/tooth]	Exp r_{CE1} [mm]	Dev.St. r_{CE1} [mm]	ΔF_y [N]	α [°]	Dev.St. α [°]	Exp r_0 [mm]	γ [rad]
1	0,0030	0,3985	0,0398	0,43	177,47	1,01	0,010	1,147
2	0,0035	0,4040	0,0104	0,37	172,26	1,57	0,028	1,257
3	0,0005	0,4133	0,0084	0,35	168,44	1,56	0,043	1,171
4	0,0065	0,4053	0,0214	0,31	175,37	3,54	0,019	0,990
5	0,0055	0,4108	0,0286	0,35	170,33	2,42	0,037	1,151
6	0,0050	0,4176	0,0290	0,38	174,55	4,50	0,029	0,690

Table 4 – Measures of r_{CE1}, ΔFy and α on LB-PBF specimen.

TEST	f_z [mm/tooth]	Exp r_{CE1} [mm]	Dev.St. r_{CE1} [mm]	ΔF_y [N]	α [°]	Dev.St. α [°]	Exp r_0 [mm]	γ [rad]
1	0,0030	0,3980	0,0242	0,11	176,74	1,56	0,012	1,281
2	0,0035	0,3948	0,0174	0,11	178,09	2,48	0,007	1,535
3	0,0005	0,3945	0,0171	0,06	178,78	2,32	0,004	1,440
4	0,0065	0,4010	0,0055	0,07	179,74	3,81	0,007	0,136
5	0,0050	0,3975	0,0198	0,08	177,82	2,49	0,008	1,195
6	0,0070	0,3998	0,0272	0,09	177,42	5,78	0,010	1,038

The standard deviation of r_{CE1} ranges between the 2% and the 10% of the nominal value. It is a not-neglectable variability due to the impact of the tool run-out phenomenon on of r_{CE1}, which is equal to few micrometres. It is a confirmation about the necessity to determine the run-out by avoiding direct measurements on the machined features, especially during the machining of soft materials where the burrs are higher and lead to a difficult measurement of the width, even if after deburring. The run-out parameter r_0 ranged between 4 and 43 micrometres, which can not be considered as reliable values due to the guarantee of the tool holder manufacturer of a maximum value of run-out equal to 3 micrometres. The low differences about the cutting force peaks ΔFy related to the tool flutes is a further demonstration of the not-reliability of the experimental determination of r_{CE1}.

The experimental values of r_{CE1} resulted averagely higher for GC sample than LB-PBF sample. In GC specimen the ΔF_y is higher while angle α is lower; both the results demonstrate that GC specimen is more subjected to run-out phenomenon instead of the LB-PBF sample. Run-out is a

random phenomenon determined by the elastic clamping of the tool in the tool holder and it does not depend on the material properties. Consequently, the novel procedure of calibration of the model was applied on two different geometrical configurations of run-out.

The implementation of the model (Eq. 13) needs the calibration of the K_{ts} variable for the AlSi10Mg alloy before the calculation of r_{CE1} values. In Table 5 the sensitivity analysis on the influence of K_{ts} value on the other terms described in Eq. 13 is presented. The analysis is presented for the data obtained with GC specimen, but analogue consideration can be exploited with the data referred to the LB-PBF sample.

Table 5 – Sensitivity analysis on K_{ts} referred to GC.

K_{ts} [N/mm^2]	$a\cdot(r_{CE1})^4$ [mm^4]	$b\cdot(r_{CE1})^3$ [mm^4]	$c\cdot(r_{CE1})^2$ [mm^4]	$e\cdot(r_{CE1})$ [mm^4]	g [mm^4]
1	4,92E-05	-2,03E-04	9,36E-03	-1,89E-02	8,29E-04
10	4,92E-05	-2,04E-05	-9,78E-02	2,02E-02	9,48E-02
100	4,92E-05	-2,04E-06	-9,89E-02	2,06E-03	9,69E-02
1000	4,92E-05	-2,14E-07	-9,89E-02	2,15E-04	9,69E-02
10000	4,92E-05	-3,07E-08	-9,89E-02	3,09E-05	9,69E-02
100000	4,92E-05	-1,24E-08	-9,89E-02	1,25E-05	9,69E-02
1000000	4,92E-05	-1,06E-08	-9,89E-02	1,07E-05	9,69E-02

As visible, the terms which assumes highest value are g and $c\cdot(r_{CE1})^2$. Common values of K_{ts} for metallic alloys are higher than 10^3 N/mm^2 thus, and in [11] it is reported a K_{ts} for AlSi10Mg alloy ranging between 10^3 N/mm^2 and 10^4 N/mm^2. Assuming this hypothesis, the order of magnitude of g and $c\cdot(r_{CE1})^2$ is 10^{-2}, while the other terms range between 10^{-4} and 10^{-8}. As conclusion, the terms of Eq. 13 $a\cdot(r_{CE1})^4$, $b\cdot(r_{CE1})^3$ and $e\cdot(r_{CE1})$ are approximated to zero. The following results were obtained supposing K_{ts} equal to 10000 N/mm^2 and simplifying the Eq. 13 from 4th to 2nd order. The result is visible in Eq. 19.

$$c \cdot {r_{CE1}}^2 + g = 0 \tag{19}$$

This 2nd grade equation leads to a simplified equation to predict r_{CE1} (Eq. 20).

$$r_{CE1} = \pm\sqrt{-\frac{g}{c}} \tag{20}$$

Where c and g can be computed with Eq. 12, Eq. 16 and Eq. 18. In Table 6 and Table 7 there is a comparison between experimental values and the data computed from the analytical model. The simplified equation (Eq. 19) is applied to predict r_{CE1} by using experimentally measured d, α, ΔF_y parameters and c, g constants. The error considered (i.e. *% error*) is calculated according to the equation Eq. 21.

$$\%\, error = \frac{|\Delta r_{CE1}|}{Analytical\, r_{CE1}} \cdot 100 \tag{21}$$

Table 6 – Comparison between experimental r_{CE1} values for GC machining tests and the computed ones.

TEST	Exp r_{CE1}[mm]	Computed r_{CE1}[mm]	Δr_{CE1} variation [mm]	% error
1	0,3985	0,3945	0,0040	1,02%
2	0,4040	0,3945	0,0095	2,42%
3	0,4133	0,3945	0,0188	4,76%
4	0,4053	0,3945	0,0108	2,73%
5	0,4108	0,3945	0,0163	4,12%
6	0,4176	0,3945	0,0231	5,86%

Table 7 – Comparison between experimental r_{CE1} values for LB-PBF machining tests and the computed ones.

TEST	Exp r_{CE1}[mm]	Computed r_{CE1} [mm]	Δr_{CE1} variation [mm]	% error
1	0,3980	0,3945	0,0035	0,89%
2	0,3948	0,3945	0,0003	0,07%
3	0,3945	0,3945	0,0000	0,00%
4	0,4010	0,3945	0,0065	1,66%
5	0,3975	0,3945	0,0030	0,77%
6	0,3998	0,3945	0,0053	1,35%

The value of r_{CE1} calculated for all the experimental tests resulted constant up to the fourth decimal place and equal to the half of the actual tool diameter (i.e., *d/2*), regardless the sample and the process parameter. The computed values of r_{CE1} changed only after the fourth decimal place. This result does not agree with the experimental measurement of r_{CE1}, but the experimental values of r_{CE1} can not be considered reliable as previously discussed.

Conclusions

The application of Eq. 19 to the experimental tests demonstrates that the procedure computes values of run-out lower than the values determined with the classic methodology. The experimental determination through the direct measurement of the channel width led in this study case to an overestimation of run-out, while the value of the computed r_{CE1} is always equal to half the tool diameter up to the 4th decimal place. As consequence, the new procedure predicts an almost null run-out in both the specimens (LB-PBF and GC). On the other hand, the differences about cutting force peaks on the two tool flutes demonstrates that tool run-out phenomenon was not completely neglectable. As a matter of fact, micro-milling of GC specimen was more affected by tool run-out. Based on those evidence, it can be stated that the estimation of tool-run parameters is still not possible by using only the cutting force signal (i.e., ΔF_y and α). Nevertheless, the obtained results have been found from a restricted dataset, due to the exclusion of the tests more affected by the presence of excessive burrs. Furthermore, the estimation of r_{CE1} could be performed by solving the 4th grade equation without doing any approximation. Future research should expand the experimental campaign to analyse more specimens, realized from different production techniques. Moreover, the specimens realized by the same production technology should be compared as a function of the heat treatment they were subjected to. It would give a larger dataset to elaborate more general conclusions on the reliability of the analytical model presented. A direct comparison between the cutting force signal predicted by the model and experimental acquired will be performed to assess the estimation of the tool run out by the new methodology.

Aknowledgment

Financed by the European Union - NextGenerationEU (National Sustainable Mobility Center CN00000023, Italian Ministry of University and Research Decree n. 1033 - 17/06/2022, Spoke 11

- Innovative Materials & Lightweighting). The opinions expressed are those of the authors only and should not be considered as representative of the European Union or the European Commission's official position. Neither the European Union nor the European Commission can be held responsible for them. CUP D83C22000690001.

References

[1] R. Yadav, N. D. Chakladar, S. Paul, A dynamic recrystallization based constitutive flow model for micro-machining of Ti-6Al-4V, J. Manuf. Process. 77 (2022) 463-484. https://doi.org/10.1016/j.jmapro.2022.03.040

[2] D. Wang, L. Penter, A. Hänel, Y. Yang, S. Ihlenfeldt, Investigation on dynamic tool deflection and run out-dependent analysis of the micro-milling process, Mech. Syst. Signal Process. 178 (2022) 109282. https://doi.org/10.1016/j.ymssp.2022.109282

[3] C. Cappellini, A. Malandruccolo, A. Abeni, A. Attanasio, A feasibility study of promoting osseointegration surface roughness by micro-milling of Ti-6Al-4V biomedical alloy, Int. J. Adv. Manuf. Technol. 126 (7-8) (2020) 3053-3067. https://doi.org/10.1007/s00170-023-11318-z

[4] A. Abeni, D. Loda, T. Özel, A. Attanasio, Analytical force modelling for micro milling additively fabricated Inconel 625, Prod. Eng. 14 (2020) 613-627. https://doi.org/10.1007/s11740-020-00980-x

[5] C. Cappellini, A. Abeni, A. Attanasio, Modelling of micro-milling by considering tool run-out and ploughing regime, Procedia CIRP, 118 (2023) 402-407. https://doi.org/10.1016/j.procir.2023.06.069

[6] G. Bissacco, H.N. Hansen, J. Slunsky, Modelling the cutting edge radius size effect for force prediction in micro milling, CIRP Ann. Manuf. Technol. 58 (2009) 49-52. https://doi.org/10.1016/j.cirp.2008.03.085

[7] P. Rodríguez, J.E. Labarga, A new model for the prediction of cutting forces in micro end-milling operations, J. Mater. Process. Technol. 213 (2013) 261–268. https://doi.org/10.1016/j.jmatprotec.2012.09.009

[8] W. Chen, X. Teng, D. Huo, Q. Wang, An improved cutting force model for micro milling considering machining dynamics, Int. J. Adv. Manuf. Technol. 93 (2017) 3005-3016. https://doi.org/10.1007/s00170-017-0706-2

[9] X. Zhang, T. Yu, W. Wang, Prediction of cutting forces and instantaneous tool deflection in micro end milling by considering tool run-out, Int. J. Mech. Sci. 136 (2018) 124-133. https://doi.org/10.1016/j.ijmecsci.2017.12.019

[10] A. Attanasio, Tool Run-Out Measurement in Micro Milling, Micromachines 8 (2017) 221. https://doi.org/10.3390/mi8070221

[11] F.O. Campos, A.L. Mougo, A.C. Araujo. Modeling micromilling cutting force on machining aluminum alloy, 22nd International Congress of Mechanical Engineering COBEM (2013).